

Simulation of premixed turbulent flames

M. Day and J. Bell

Center for Computational Science and Engineering, Lawrence Berkeley National Laboratory,
Berkeley, CA, 94720

E-mail: MSDay@lbl.gov

1. Introduction

Premixed turbulent flames are of increasing practical importance and remain a significant research challenge in the combustion community. These flames have the potential to operate cleanly and efficiently over a broad range of fuels, and therefore to represent a key element in the implementation of low-emissions burners for a variety of industrial applications. However, it is difficult to design lean premixed systems that are both safe and reliable. Premixed systems require device-scale flame stabilization techniques to create a statistically stationary configuration, and at the same time operate in regimes where the dynamics of the inertial scales of the turbulence, and the interactions of the turbulence with the combustion chemistry have significant effect on the flame propagation. Considerable effort has been made within the community to correlate experimental data from different configurations (see [1–5], for example) in terms of parameters that are device-independent. However, to date those type of correlations have remained elusive and data appears to be sensitive to the flow configuration.

Simulation has the potential to overcome the limitations of theory and experiment and provide new insights into the behavior of premixed flames. Our objective is to perform “first principles” simulations that incorporate detailed descriptions of chemistry and transport without the use explicit models for turbulence or turbulence/chemistry interaction. As examples here, we consider two turbulent premixed methane flame experiments: a V-flame anchored on a thin rod spanning a circular nozzle, and a piloted Bunsen flame anchored on a rectangular nozzle. These flames span a broad range and spatial and temporal scales. Simulation domains must be comparable to the window of the experimental diagnostics (order $O(10)$ cm on side), while resolving the structure of the flame front that is less than 1 mm wide. Resolution requirements for the turbulent flow are less stringent but vary throughout the domain. Acoustic waves propagate at 10^5 cm/s in the hot products while typical fluid velocities are $O(10^3)$ cm/s. With no turbulence present the flames overtake fuel at a laminar flame speed of 15-40 cm/sec.

We have developed numerical methodology that combines a low-Mach number formulation combined with adaptive mesh refinement to exploit the variation of scales associated with premixed flame simulations. This combined approach, when implemented on parallel computing hardware, improves computational efficiency by several orders of magnitude. The reader is referred to [6] for details of the low Mach number model and its numerical implementation.

To carry out these simulations, our strategy is to characterize independently the turbulence generation process using integral scale and turbulent intensity data measured in the experiment. We then impose the inflow turbulence as a time-dependent boundary conditions for the reacting flow evolution. For these investigations, we use the DRM-19 subset of the GRI-Mech 1.2 methane mechanism [7] for detailed transport and chemical kinetics (DRM-19 contains 20 chemical species

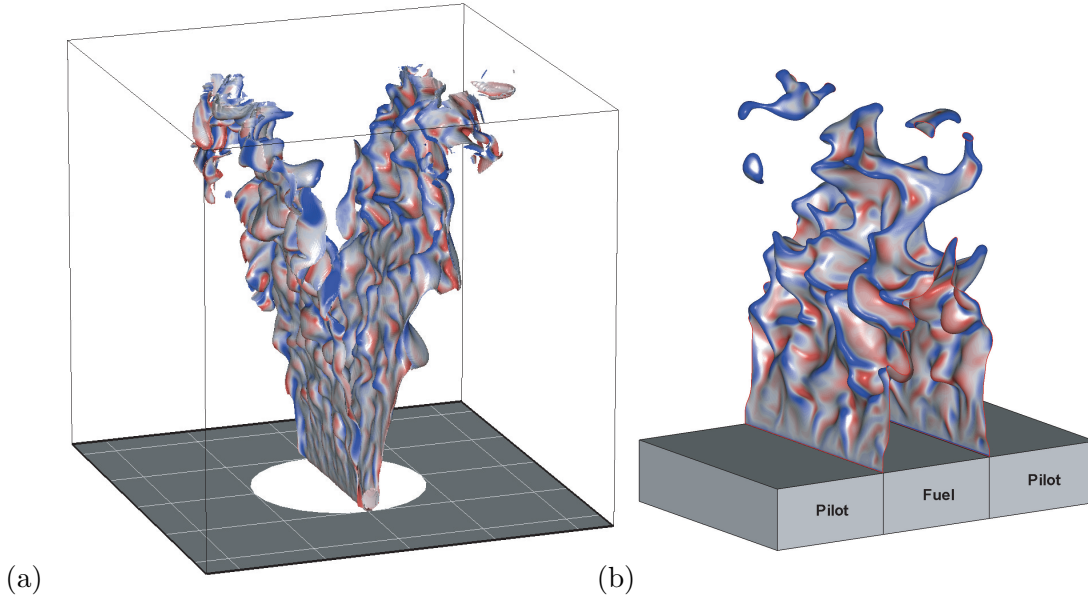


Figure 1. Instantaneous computed flame surfaces for (a) the V-flame, and (b) the slot Bunsen flame, colored by mean flame surface curvature. The V-flame inlet nozzle is 5 cm in diameter; the simulation domain was 12 cm on a side. The fuel duct in the Bunsen flame is 2.5×5 cm, as are the two pilot burners; the simulation domain was approximately $7.5 \times 5 \times 12.7$ cm high.

and 84 fundamental reactions). Details of the simulation strategy as well as the refinement strategy for each of the cases is discussed in [8] and [9] for the V-flame and slot flame cases, respectively.

2. Simulations results and experimental comparisons

A 3D view of the instantaneous flame surfaces for both simulations appears in Fig. 1. The V-flame surface is indicated by an isosurface, $\|\nabla T\| = 10^6$ K/m, and colored red (blue) where local value of mean curvature is positive (negative). Here the curvature is positive if the center of curvature is in the products, and negative if in the fuel. It is evident that the surface perturbations grow considerably as the flow advects downstream of the stabilizing rod. Very far downstream, the flow interacts strongly with the external environment, generating very large scale surface perturbations. The instantaneous flame surface from the Bunsen flame calculation (given here by the $T=1685$ K isotherm) shows that the pre-mixture issuing from the central slot ignites on contact with

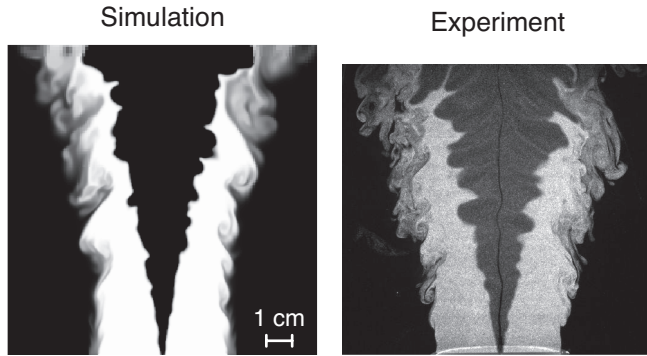


Figure 2. Computed CH_4 mole fraction and typical Mie scattering image for the V-flame (see Ref. [8] for details).

the hot, stabilizing coflows to form two flame sheets anchored at each lip. Above 1 cm, the flame sheets exhibit the crenelated (cusped) texture characteristic of premixed flames in mild turbulence, as seen in the V-flame. Sharp ridges of high negative curvature surround large pockets of

modest positive curvature; these features are more pronounced here than in the V-flame. The thin ridges are the dominant feature of the flame as the two flame sheets merge at the flame tip. The elevation where the two sheets merge changes with the shape of the ridges and fluctuates rapidly, varying from 4 to 6 cm along the slot. The ridges often burn through to detach portions of the flame surface.

A typical centerline slice of the methane concentration obtained from the V-flame simulation is shown on the left in Fig. 2. Experimentally, the instantaneous flame location is determined

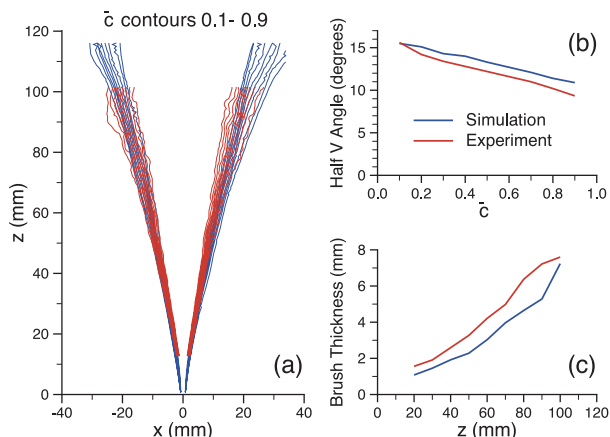


Figure 3. Comparison of mean progress for the V-flame: (a) \bar{c} contours; (b) flame half-angle (from vertical) as a function of \bar{c} ; (c) Flame brush thickness.

using the large differences in Mie scattering intensities from the reactants and products to clearly outline the flame (Fig. 2 right). We see that the wrinkling of the flame in the experiment and the computation is similar in size and structure. The different fine-scale structure on the outer edge of the fuel stream may be related to the difference in the dynamics of fuel versus particles, or may be a result of under-resolution in the region of the flow which is not refined to the finest level.

For the V-flame, contours of the mean reaction progress, \bar{c} are depicted in Fig. 3a, where $\bar{c} = 0$ in reactants, and $\bar{c} = 1$ in the products. The angle between \bar{c} contours and the vertical is plotted in Fig. 3b. For $\bar{c} = 0.5$ the simulation predicts a flame angle of 13.4° compared

to 12.2° for the experiment representing a 10% overestimate of the flame angle. The downstream growth rate of the flame brush thickness is plotted in Fig. 3c.

A comparison of instantaneous flames slices for the Bunsen flame are presented in Fig. 4. The flame brushes for this case are shown in Fig. 5. The experiment and the simulation both have an average flame height of approximately 4 cm. Measuring the length of the $\bar{c} = 0.5$ contour from the simulation data, we can define a global turbulent flame speed as the average consumption speed over this area required to consume the fuel. This gives a result of $2.45 \times s_L$ compared to $2.55 \times s_L$ for the experimental data. (See [5] for details of how the turbulent flame speed is computed for the experimental data.) The width of the flame brush (defined as the full width half maximum of c'_{rms}) was computed both from the experimental data, and from the binarized simulation data. Along the flanks of the flame, the two measures agree remarkably well, increasing linearly from 2 mm at an elevation of 1 cm to approximately 11 mm at 3.5 cm. Agreement in flame brush thickness profiles shows that the simulation is correctly capturing the fluctuating flame surface dynamics on the longer timescale associated with turbulent structure advection.

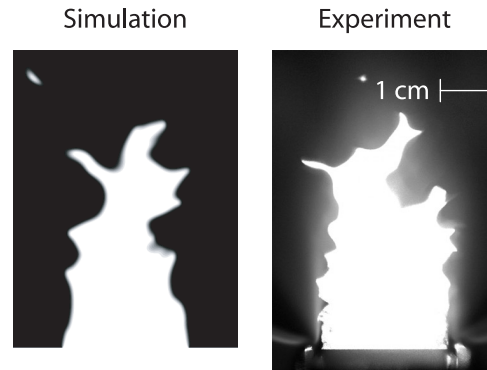


Figure 4. Computed CH_4 mole fraction and typical Mie scattering image for the Bunsen flame (see Ref. [9] for details).

3. Discussion

Although the simulation and experiment show satisfactory agreement, there are notable differences in both cases. Identifying the origin of these differences is a complex issue; there are a wide variety of currently irreducible sources of discrepancy between the simulation and data from experimental diagnostics. Based on an examination of the two case studies discussed above we can identify four broad sources of “errors” in performing these types of simulations.

Models and Numerics. Errors in the the mathematical description of the fluid-dyanmical system are perhaps the simplest to keep under control. Numerical convergence may be investigated systematically by adjusting refinement criteria and methodically reducing spatial and temporal resolution. The low Mach number approximation can be validated with fully compressible simulations for test cases accessible to both approaches.

A related issue is the relationship between the level of physics fidelity and the accuracy of the resulting simulations. We have used a mixture model for transport; our chemical mechanism is a reduced mechanism of intermediate complexity; we have used an optically thin approximation to radiation. In each of these cases both higher and lower fidelity approximations are available but it is largely unknown how sensitive solutions are to changes in the models in turbulent simulations.

Data. A considerable level of investigation in the combustion community is dedicated to improving the chemical model. In spite of its importance, there are significant errors in some of these models. For example, the GRIMech-3.0 mechanism for natural gas was optimized for a number of experimental “targets”, however, for lean flames the mechanism overpredicts flame speed by as much as 20%. The errors in flame angle for the V-flame are consistent with this error in flame speed. Larger errors are known to exist for more detailed subprocesses, such as the production of prompt NO_x .

Configuration. Several sources of error arise primarily because we are unable to simulate the entire experimental system. For example, in the simulations discussed in this paper, pre-computed turbulent fluctuations were superimposed over the mean inlet flow. These fluctuations were generated to match the experimental characterizations, which include r.m.s. fluctuation intensity and integral scale length. However, the spectra are otherwise unspecified, and may contain significant artifacts of the turbulence generation mechanism and nozzle wall boundary conditions as well as other large scale effects due to the fuel/oxidizer plumbing, etc. Similarly, we need to specify boundary conditions on the other parts boundary of the computational domain that reflect how the laboratory environment responds to the flame. Typically no information to help characterize this response is available. Analysis of the slot burner simulations show that the mean flame shape is sensitive to details of the boundary conditions suggesting that differences in the specification are likely responsible for the observed differences in flame brush shape.

Diagnostics. Typical experimental “diagnostics” actually involve a considerable list of assumptions about the flame or flow. For example the images discussed above implicitly identify the flame with a given isotherm and are analyzed assuming that key 3-D structures can be inferred from 2-D slices. Laser-induced fluorescence (LIF) intensity, frequently used as a non-intrusive technique for quantitative measurements of flame intermediates, depends on

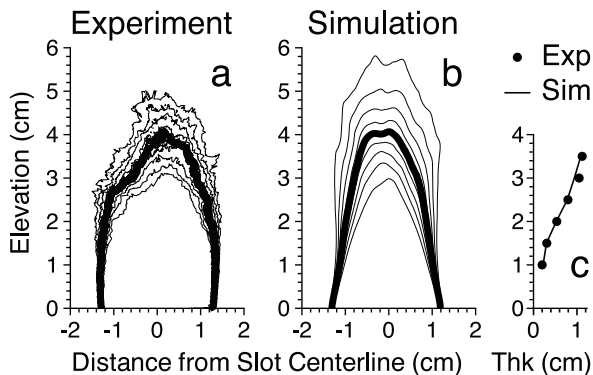


Figure 5. Comparison of reaction progress for the Bunsen flame: (a) experimental \bar{c} based on Mie scattering data; (b) computed \bar{c} based on the fluid density, (c) Flame brush thickness comparison as a function of height from the burner surface.

the number density of the excitable molecules, spectral signal absorption, and the fluorescence quantum yield which includes decay rates due to spontaneous emission and electronic quenching that depend strongly on the distribution of many of the other chemical species in the system. Deconvolution of measured LIF signals requires *a priori* knowledge of temperature and the species mole fractions that can only be roughly estimated.

4. Conclusions

Recent advances in numerical methodologies and hardware have made it possible to perform “first principles” simulations of turbulent premixed laboratory flames. However, the simulations alone suffer significant shortcomings when we wish to use them to understand basic flame physics. Rather these new simulation capabilities open the door to new more effective collaborations between experimentalists, chemists, mathematicians and theorists. An analysis of potential sources of discrepancy between simulation and experiment reveals opportunities to collaborate on design of experiments that are better characterized, development of improved diagnostic methodologies and improved chemical models that provide more accurate descriptions of chemistry and transport. Furthermore, we can strengthen the linkages between the complex multi-species phenomena in real flames and theoretical models that enable a more complete understanding of the processes.

Acknowledgments

This work was supported by the SciDAC Program of the DOE Office of Mathematics, Information, and Computational Sciences under contract No. DE-AC02-05CH11231. Simulations of the V-flame were carried out in collaboration with Robert Chang and Ian Shepherd at LBNL. The Bunsen flame simulations were carried out in collaboration with Jim Driscoll (University of Michigan) and Sergei Filatyev (Purdue University). All simulations presented were run on the NERSC Bassi machine at Lawrence Berkeley National Laboratory.

References

- [1] S. S. Sattler, D. A. Knaus, and F. C. Gouldin. Determination of three-dimensional flamelet orientation distributions in turbulent V-flames from two-dimensional image data. *Proc. Combust. Inst.*, 29:1785–1795, 2002.
- [2] I. G. Shepherd, R. K. Cheng, T. Plessing, C. Kortschik, and N. Peters. Premixed flame front structure in intense turbulence. *Proc. Combust. Inst.*, 29:1833–1840, 2002.
- [3] D. Most, F. Dinkelacker, and A. Leipertz. Lifted reaction zones in premixed turbulent bluff-body stabilized flames. *Proc. Combust. Inst.*, 29:1801–1806, 2002.
- [4] Y.-C. Chen, P. A. M. Kalt, R. W. Bilger, and N. Swaminathan. Effects of mean flow divergence on turbulent scalar flux and local flame structure in premixed turbulent combustion. *Proc. Combust. Inst.*, pages 1863–1871, 2002.
- [5] S. A. Filatyev, J. F. Driscoll, C. D. Carter, and J. M. Donbar. A database of turbulent premixed flame properties for model assessment, including burning velocities, stretch rates, and surface densities. *Combust. Flame*, 141:1–21, 2005.
- [6] M. S. Day and J. B. Bell. Numerical simulation of laminar reacting flows with complex chemistry. *Combust. Theory Modelling*, 4:535–556, 2000.
- [7] M. Frenklach, H. Wang, M. Goldenberg, G. P. Smith, D. M. Golden, C. T. Bowman, R. K. Hanson, W. C. Gardiner, and V. Lissianski. GRI-Mech—an optimized detailed chemical reaction mechanism for methane combustion. Technical Report GRI-95/0058, Gas Research Institute, 1995. http://www.me.berkeley.edu/gri_mech/.
- [8] J. B. Bell, M. S. Day, I. G. Shepherd, M. Johnson, R. K. Cheng, J. F. Grcar, V. E. Beckner, and M. J. Lijewski. Numerical simulation of a laboratory-scale turbulent V-flame. *Proc. Natl. Acad. Sci. USA*, 102(29):10006–10011, 2005.
- [9] J. B. Bell, M. S. Day, J. F. Grcar, M. J. Lijewski, J. F. Driscoll, and S. A. Filatyev. Numerical simulation of a laboratory-scale turbulent slot flame. *Proc. Combust. Inst.*, 31, 2006. to appear.